Modified Perturb and Observe MPPT Algorithm for Drift Avoidance in Photovoltaic Systems

Muralidhar Killi and Susovon Samanta, *Member, IEEE*

***Abstract*—The perturb and observe (P&O) maximum power point tracking (MPPT) algorithm is a simple and efficient tracking technique. However, the P&O tracking method suffers from drift in case of an increase in insolation (G), and this drift effect is severe in case of a rapid increase in insolation. Drift occurs due to the incorrect decision taken by the conventional P&O algorithm at the first step change in duty cycle during increase in insolation. A modified P&O technique is proposed to avoid the drift problem by incorporating the information of change in current (ΔI) in the decision process in addition to change in power (ΔP) and change in voltage (ΔV). The drift phenomena and its effects are clearly demonstrated in this paper for conventional P&O algorithm with both fixed and adaptive step size technique. A single-ended primary inductance converter is considered to validate the proposed drift-free P&O MPPT using direct duty ratio control technique. MATLAB/Simulink is used for simulation studies, and for experimental validation, a microcontroller is used as a digital platform to implement the proposed algorithm. The simulation and experimental results showed that the proposed algorithm accurately tracks the maximum power and avoids the drift in fast changing weather conditions.**

***Index Terms*—Drift phenomena and single-ended primary inductance converter (SEPIC), maximum power point tracking (MPPT), perturb and observe (P&O), photovoltaic (PV).**

I. Introduction

PHOTOVOLTAIC (PV) power generation is evolving as one of the most remarkable renewable energy sources because of its benefits like ecofriendly nature, less maintenance, and no noise. The characteristics of a PV module will alter with solar insolation level and atmospheric temperature [1]–[3]. The efficiency of the PV system primarily depends on the operating point on the characteristic curve of the PV module. Maximum power point tracking (MPPT) is one of the vital functions that every PV system should include. Until now, a large number of MPPT techniques have been developed [4]–[26] to increase the efficiency of the PV system. MPPT algorithms such as fractional open-circuit voltage [4], fractional short-circuit current [4], hill-climbing [5], perturb and observe (P&O) [6]–[13], incremental conductance (IncCond) [14]–[18], incremental resistance (INR) [19], ripple correlation control (RCC) [20], fuzzy logic [21], neural network [22], particle swarm optimization (PSO) [23], [24], and sliding mode [25], [26] techniques are some of the MPPT techniques available in the literature. The overview of various MPPT techniques is discussed in [27]–[30].

This paper focuses on a widely used P&O algorithm because of its advantages, e.g., it is PV array independent, it is a true MPPT, it can be implemented in both analog and digital platforms, it does not require periodic tuning, and it is easy to implement [29]. The P&O technique is developed by checking the slope (dP/dV) on the P–V characteristics of the PV module. The slope $(dP/dV) > 0$ at the left of MPP and $(dP/dV) < 0$ at the right of MPP. Thus, depending on the sign of the slope, the operating voltage has to be perturbed to track the peak power. It is reported in the literature that P&O can be implemented either by using voltage reference control with the help of a proportional-integral (PI) controller [11] or by using direct duty ratio control [12]. The tracking performance of the P&O is determined by the tracking time and steady-state oscillations which depend on the perturbation step size. A smaller perturbation step size results in lower oscillations but results in a slower response. On the other hand, a large perturbation step size increases the steady-state oscillations [10]. Later to improve the performance of P&O, a variable perturbation step size is utilized in [5], [7], and [12].

Although P&O has remarkable advantages, the sudden change in atmospheric conditions causes this P&O algorithm to drift away from MPP [27], and the analysis of this drift problem is given in [11] and [31]. This paper presents a clear analysis of drift such as when the drift can occur, the movement of the operating point, and the effect of drift in case of one time insolation change, as well as rapid change in insolation. The drift phenomena in case of the adaptive P&O technique are also incorporated in this paper.

The solution to avoid the drift problem is given in [6] by applying a constraint on perturbation step size (ΔD). However, to avoid the drift for a large change in insolation, a high value of ΔD is required, which will effectively increase the power loss in steady state. In [9], the solution to the drift is given by considering upper and lower threshold limits to change in power (ΔP) and is not an optimal solution due to the constraints on the threshold values of ΔP, which are mainly dependent on the amount of change in insolation. Another solution in the name of full curve evaluation is presented in [8] by evaluating the entire trend in P–V curve, but it is not possible to evaluate the entire trend in P–V curve in case of a rapid change in

Manuscript received May 18, 2014; revised September 27, 2014 and November 30, 2014; accepted January 15, 2015. Date of publication February 27, 2015; date of current version August 7, 2015.

The authors are with the Department of Electrical Engineering, National Institute of Technology, Rourkela 769008, India (e-mail: samantas@nitrkl.ac.in).

Color versions of one or more of the figures in this paper are available online at http://ieeexplore.ieee.org.

Digital Object Identifier 10.1109/TIE.2015.2407854

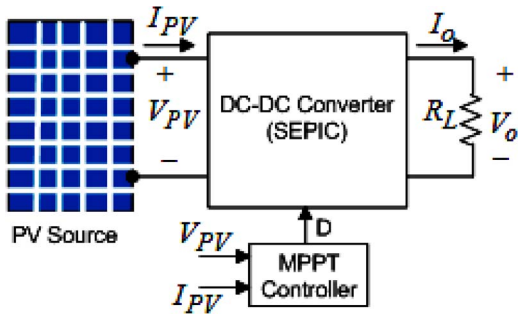

Fig. 1. Block diagram of the PV system with MPPT control.

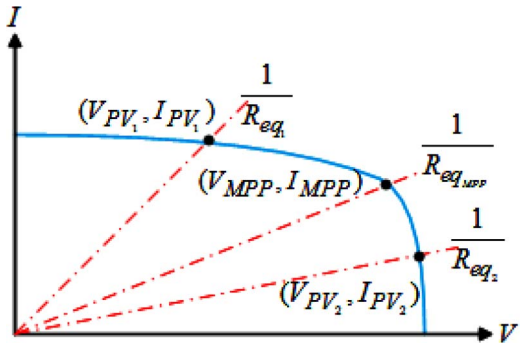

Fig. 2. Variation of operating point with respect to load line $(R_{\rm eq})$.

insolation as the operating point moves into the new point on the corresponding insolation curve for each insolation change. This paper presents an accurate and simple solution to this drift problem by evaluating another parameter, i.e., change in current (ΔI) by modifying the conventional P&O MPPT algorithm.

A dc–dc converter acts as an interface to operate at MPP by changing the duty cycle (D) of the converter. Different converter topologies such as buck [8], boost [30], buck–boost [23], Cuk [32], and single-ended primary inductance converter (SEPIC) [26], [32] are available to use in the stand-alone PV system for battery charger and other applications. In this paper, a SEPIC converter is considered to validate the proposed drift-free P&O MPPT algorithm, and it can be applicable to any other converter topology.

II. Conventional P&O MPPT

The operating point on the characteristics of the PV module primarily depends on the impedance matching of the PV module with respect to the connected load. A dc–dc converter between the PV module and the load acts as an interface to operate at MPP by changing the duty cycle of the converter generated by the MPPT controller, and a general block diagram of the PV system is shown in Fig. 1.

Using input and output voltage relation for SEPIC (i.e., $V_o = (D/1-D)V_{\rm PV}$), the efficiency of the converter can be expressed by (1)

$$\left.\begin{aligned} \eta &= \frac{V_o I_o}{V_{\rm PV} I_{\rm PV}} \\ \eta &= \frac{V_o I_o}{V_{\rm PV}^2/R_{\rm eq}} = \left(\frac{V_o}{V_{\rm PV}}\right)^2 \frac{R_{\rm eq}}{R_L} = \left(\frac{D}{1-D}\right)^2 \frac{R_{\rm eq}}{R_L} \end{aligned}\right\} \quad (1)$$

where $V_{\rm PV}$ and $I_{\rm PV}$ are the PV voltage and current, respectively. The equivalent input resistance $(R_{\rm eq})$ of the converter as seen by the PV module can be obtained from (1) as follows:

$$R_{\rm eq} = \eta \left(\frac{1-D}{D}\right)^2 R_L. \quad (2)$$

From (2), it can be noticed that, by changing the duty cycle, the operating point can be changed as $R_{\rm eq}$ changes, as shown in Fig. 2, and the MPPT controller should change the duty cycle in order to track the peak power.

The conventional P&O MPPT algorithm is developed based on the slope (dP/dV) variation on the P–V characteristics of the PV module. From the P–V characteristics shown in Fig. 3, it can be visualized that the slope is positive at the left of MPP and negative at the right of MPP. Depending on the sign of the slope, the duty cycle has to be perturbed in order to track the peak power, and the flowchart of this conventional P&O MPPT algorithm is shown in Fig. 4. The duty cycle and the PV voltage $(V_{\rm PV})$ are inversely proportional to each other, i.e., an increase in duty cycle causes the $V_{\rm PV}$ to decrease and vice versa.

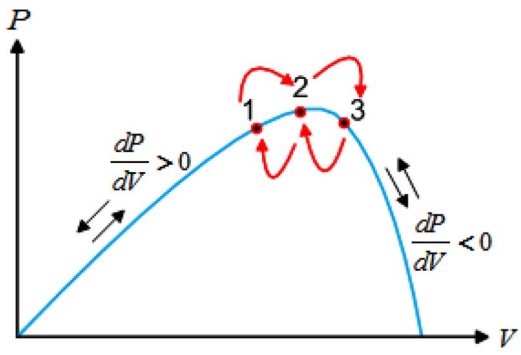

Fig. 3. Slope (dP/dV) variation and steady-state three-level operation of P&O MPPT.

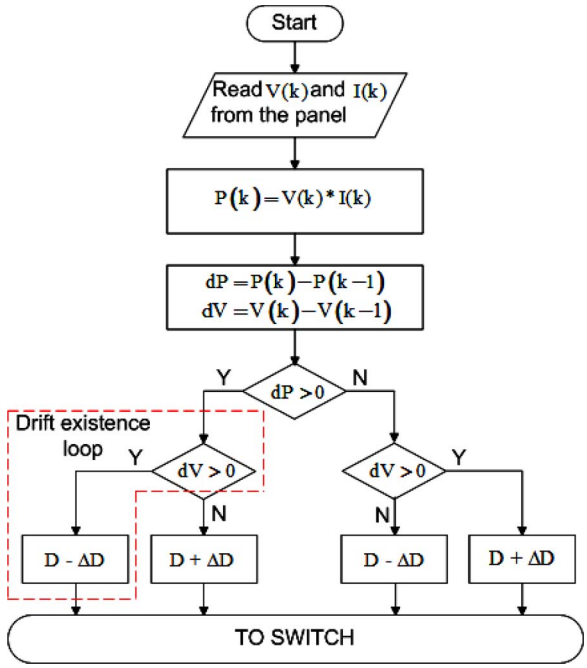

Fig. 4. Flowchart of the conventional P&O MPPT algorithm.

The two vital parameters in any MPPT algorithm are perturbation time and perturbation step size, and the criteria for choosing these two parameters are described as follows.

1) Selecting Proper Perturbation Time (T_a): To make sure minimum number of oscillations with P&O algorithm (i.e., three-level operation), the perturbation time should be higher than the settling time of the system for a step change (ΔD) in duty cycle [6]. The settling time is proportional to the perturbation step size (ΔD). In the view of the adaptive technique, the perturbation time should be chosen such that it is greater than the settling time for a maximum step ($\Delta D_{\max}$) change in duty cycle.

2) Selecting Proper Perturbation Step Size (ΔD): The perturbation step size can be chosen by considering dynamic performance and steady-state performance. The maximum value of step size ($\Delta D_{\max}$) improves the dynamic performance, whereas the minimum value of step size ($\Delta D_{\min}$) improves the steady-state performance. The step size $\Delta D_{\min}$ should be chosen based on the tracking accuracy in steady state [7] and ADC resolution [12] of the microcontroller used in the system. In general, as the switching converter intrinsically contains switching ripple on the PV voltage, an optimum value of ΔD should be chosen, such that the voltage variation due to perturbation of D (ΔD) should be greater than the amplitude of the switching ripple of the PV voltage [6].

The effectiveness of the P&O technique is determined by its steady-state behavior, drift phenomena, and tracking time which are described as follows.

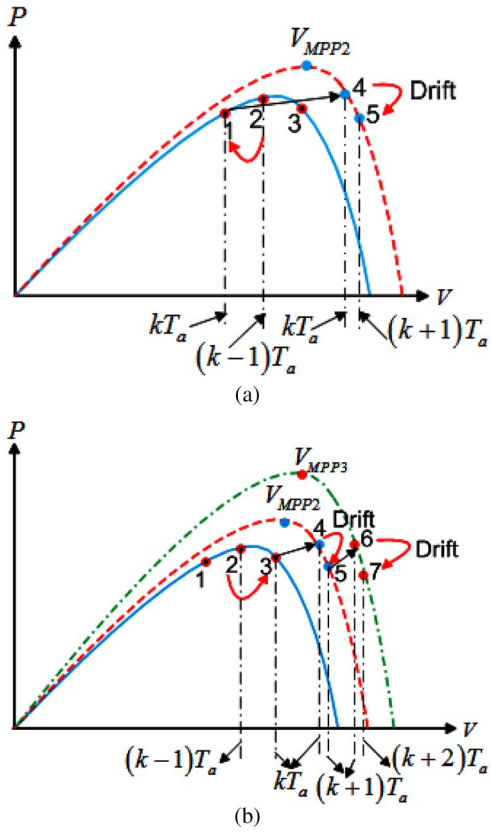

Fig. 5. Conventional P&O MPPT drift analysis. (a) Drift from point 1. (b) Drift in case of rapid increase in insolation.

A. Steady-State Three-Level Operation

The three-level operation of the P&O technique [6], [11] in steady state is depicted in Fig. 3. Assume that the operating point has been moved from point ① to point ② and the decision has to be taken at point ② by considering the values of dP and dV. As $dP = (P_2 - P_1) > 0$ and $dV = (V_2 - V_1) > 0$, the algorithm decreases the duty cycle, and hence, the operating point moves to point ③. At point ③, as $dP = (P_3 - P_2) < 0$ and $dV = (V_3 - V_2) > 0$, the algorithm increases the duty cycle, and thereby, the operating point moves back to point ②. At point ②, as $dP = (P_2 - P_3) > 0$ and $dV = (V_2 - V_3) < 0$, the algorithm increases the duty cycle, and hence, the operating point moves to point ①. At point ①, as $dP = (P_1 - P_2) < 0$ and $dV = (V_1 - V_2) < 0$, the algorithm decreases the duty cycle, and thereby, the operating point moves back to point ②. In this pattern, the algorithm makes the operating point oscillate in three points surrounding the MPP.

B. Drift Analysis

The drift problem occurs for an increase in insolation, and it will be severe for a rapid increase in insolation which generally occurs in cloudy days [6]. Drift can occur from any of the three steady-state points as shown in Fig. 5 depending on the instant of change in insolation in between the perturbation time (T_a) interval. The drift problem is due to the lack of knowledge in knowing whether the increase in power ($dP > 0$) is due to perturbation or due to an increase in insolation. Suppose that there is an increase in insolation while operating at point ① as shown in Fig. 5(a); then, the operating point will be settled to a new point ④ in the corresponding insolation curve during the same kT_a perturbation interval. Now at point ④, as $dP = P_4(kT_a) - P_2((k-1)T_a) > 0$ and $dV = V_4(kT_a) - V_2((k-1)T_a) > 0$, the algorithm decreases the duty cycle, thereby moving to point ⑤ away from the MPP in the new curve which is called drift. Similarly, for an increase in insolation at point ② and point ③, the drift problem occurs due to confusion of this conventional P&O MPPT technique. This drift problem will be severe in case of a rapid increase in insolation as shown in Fig. 5(b) and in case of adaptive P&O, as ΔD is large for a change in insolation which will result in the operating point moving in a wrong direction far away from the MPP as described as follows.

1) Effect of Drift on Adaptive P&O: The tracking time and the steady-state performance mainly depend on the perturbation step size (ΔD). To improve both steady state and dynamic performances of the P&O algorithm, an adaptive step size is chosen in [8], [14], and [33]. The duty ratio with adaptive step size can be realized as follows [8], [14]:

$$D(k) = D(k-1) \pm M * \left| \frac{dP}{dV} \right|. \tag{3}$$

From (3), it can be observed that, for an increase or decrease in insolation, the adaptive technique generates a large value of ΔD depending on the value of dP/dV. Thus, the effect of drift

will be more on adaptive P&O for an increase in insolation due to the large value of generated ΔD.

III. Drift-Free Modified P&O MPPT

The conventional P&O MPPT is developed based on the observation of dP and dV by considering the P–V characteristics of the PV module. As said previously, P&O has a demerit of drift in case of a rapid increase in insolation due to confusion, and this confusion can be eliminated by evaluating another parameter dI (change in current). The change in operating point on I–V characteristics due to a change in insolation is described as follows.

The relation between $I_{\rm PV}$ and $V_{\rm PV}$ corresponding to the present operating point on the I–V characteristics of the PV module shown in Fig. 2 can be expressed in terms of the slope of the load line as given in the following:

$$I_{\rm PV} = \frac{D^2}{\eta R_L (1-D)^2} V_{\rm PV}. \tag{4}$$

From the practical single-diode model of the PV module, the current and voltage relationship can be described as follows [3]:

$$I_{\rm PV} = I_{\rm sc} - I_o \left(e^{\frac{V_{\rm PV}}{aV_t}} - 1 \right) - \frac{V_{\rm PV} + R_s I_{\rm PV}}{R_{\rm sh}} \tag{5}$$

where $I_{\rm sc}$ is the short-circuit current of the PV module, I_o is the reverse saturation current, a is the diode ideal factor, V_t is the thermal voltage, R_s is the series resistance, and $R_{\rm sh}$ is the shunt resistance of the PV module. By substituting (4) into (5) and by considering Taylor's series expansion up to first order, (5) can be expressed as follows:

$$V_{\rm PV} \frac{D^2}{\eta R_L (1-D)^2} = I_{\rm sc} - I_o \frac{V_{\rm PV}}{aV_t} - \frac{V_{\rm PV}}{R_{\rm sh}} - \frac{R_s}{R_{\rm sh}} \frac{D^2}{\eta R_L (1-D)^2} V_{\rm PV} \tag{6}$$

and by simplifying (6), $V_{\rm PV}$ can be expressed in terms of $I_{\rm sc}$ for an insolation G and the slope of the load line as follows:

$$V_{\rm PV}|_G = \frac{I_{\rm sc}|_G}{\frac{D^2}{\eta R_L (1-D)^2} \left(1 + \frac{R_s}{R_{\rm sh}} \right) + \frac{I_o}{aV_t} + \frac{1}{R_{\rm sh}}}. \tag{7}$$

Substituting (7) into (4) yields

$$I_{\rm PV}|_G = \frac{D^2}{\eta R_L (1-D)^2} \frac{I_{\rm sc}|_G}{\frac{D^2}{\eta R_L (1-D)^2} \left(1 + \frac{R_s}{R_{\rm sh}} \right) + \frac{I_o}{aV_t} + \frac{1}{R_{\rm sh}}}. \tag{8}$$

$I_{\rm sc}$ at an insolation of G can be expressed in terms of short-circuit current at nominal conditions ($I_{{\rm sc},n}$) as follows [3]:

$$I_{\rm sc}|_G = \left(I_{{\rm sc},n} + K_I \Delta_T \right) \frac{G}{G_n} \tag{9}$$

where K_I is the short-circuit current/temperature coefficient and $\Delta_T = T - T_n$ (T and T_n are the actual and nominal temperatures, respectively). By substituting (9) in (7) and (8) and then by considering the derivatives of $V_{\rm PV}$ and $I_{\rm PV}$ with respect to insolation, the effect of change in insolation on $V_{\rm PV}$ and $I_{\rm PV}$ can be obtained by (10) and (11), respectively

$$\frac{dV_{\rm PV}}{dG} = \frac{(I_{{\rm sc},n} + K_I \Delta_T) \frac{1}{G_n} + K_I \frac{G}{G_n} \frac{dT}{dG}}{\frac{D^2}{\eta R_L (1-D)^2} \left(1 + \frac{R_s}{R_{\rm sh}} \right) + \frac{I_o}{aV_t} + \frac{1}{R_{\rm sh}}} > 0 \tag{10}$$

$$\frac{dI_{\rm PV}}{dG} = \frac{D^2}{\eta R_L (1-D)^2} \frac{(I_{{\rm sc},n} + K_I \Delta_T) \frac{1}{G_n} + K_I \frac{G}{G_n} \frac{dT}{dG}}{\frac{D^2}{\eta R_L (1-D)^2} \left(1 + \frac{R_s}{R_{\rm sh}} \right) + \frac{I_o}{aV_t} + \frac{1}{R_{\rm sh}}} > 0. \tag{11}$$

The temperature variation is proportional to the change in insolation, i.e., $(dT/dG) > 0$. In (10) and (11), the numerator is a positive value as $I_{{\rm sc},n}$, K_I, Δ_T, and dT/dG are all positive, and the denominator is also a positive quantity. Thus, conditions $(dV_{\rm PV}/dG) > 0$ and $(dI_{\rm PV}/dG) > 0$ are valid. Hence, from (10) and (11), it can be noticed that, for an increase in insolation, both $V_{\rm PV}$ and $I_{\rm PV}$ increases. Thus, with the information of ΔV and ΔI, the drift phenomena can be avoided by detecting the increase in insolation.

The I–V characteristics of the PV module and the change in operating point due to an increase in insolation are shown in Fig. 6(a). As shown in Fig. 6(a), supposing that there is an increase in insolation while operating at point ③, then the operating point will settle to a new point ④ in the new insolation curve. Now, the decision has to be taken by the algorithm at point ③, where $dI = I_4(kT_a) - I_2((k-1)T_a) > 0$ as shown in Fig. 6(a). At the same time on the $P-V$ characteristics at point ④, both $dP = P_4(kT_a) - P_2((k-1)T_a) > 0$ and $dV = V_4(kT_a) - V_2((k-1)T_a) > 0$ as shown in Fig. 6(b). Thus, all three parameters dP, dV, and dI are positive at point ④ as shown in Figs. 6(a) and (b). Thus, the positive value of dP is due to whether perturbation or due to increase in insolation can be detected by using the additional parameter dI. From the I–V characteristics, it can be observed that the two parameters both dV and dI can never have the same sign for a single insolation. Both dV and dI will be positive only for an increase in insolation as shown in Fig. 6(a). Thus, an increase in insolation can be detected by using the additional parameter dI, and thereby, increasing the duty cycle (decreasing the operating voltage), where both dV and dI are positive, can eliminate the drift problem by moving the operating point closer to the MPP as shown in Fig. 6(b). Similarly, for an increase in insolation at point ① and at point ②, the drift problem can be solved by incorporating dI into the algorithm, and the movement of the operating point with the proposed drift-free modified P&O MPPT technique in case of a rapid increase in insolation is shown in Fig. 6(c). The flowchart of this drift-free modified P&O MPPT technique is shown in Fig. 7.

IV. Simulation Results

The PV module is modeled by using the circuit model [3], and for simulation studies, the five parameters of the single-diode model for modeling of the PV module at nominal conditions are chosen as $I_{{\rm PV},n} = 1.9$ A, $I_0 = 23.089.10^{-8}$ A, $a = 1.3$, $R_s = 0.32\ \Omega$, and $R_p = 120\ \Omega$. The components for

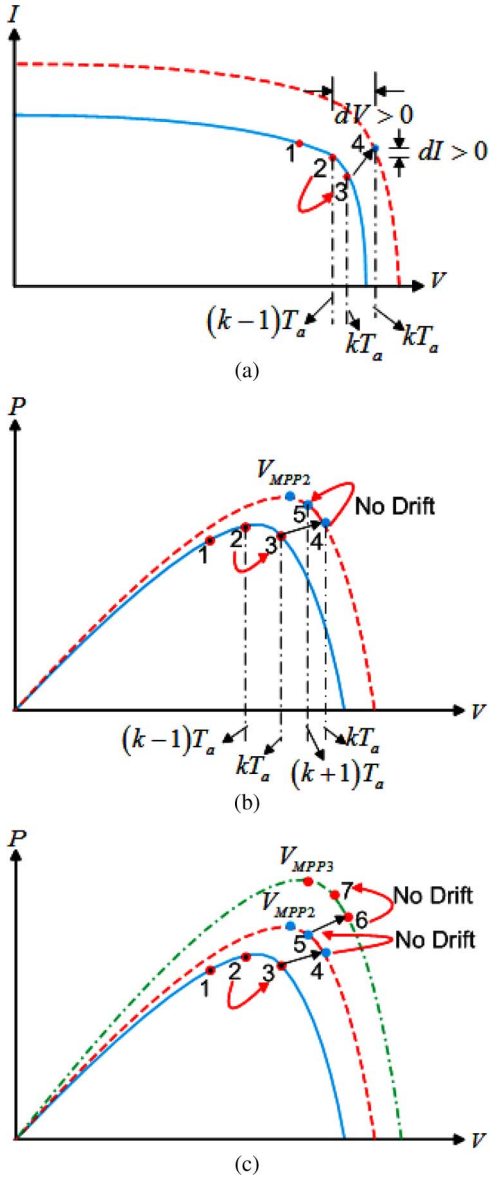

Fig. 6. Drift-free analysis with modified P&O MPPT. (a) Observation of change in current (dI). (b) One time increase in insolation. (c) Rapid increase in insolation.

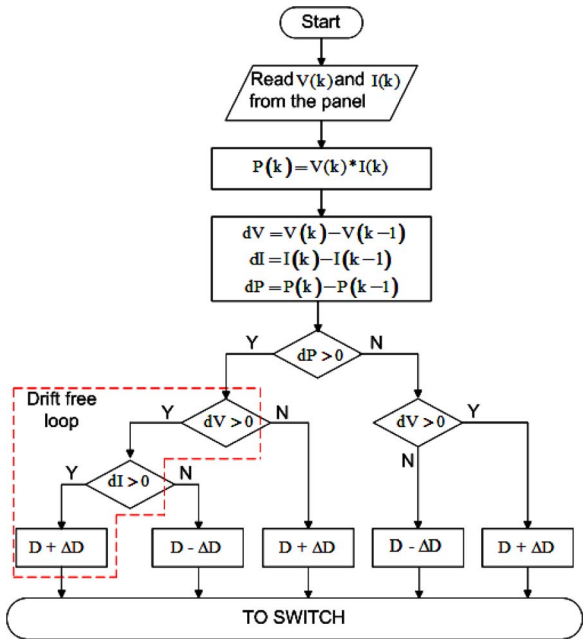

Fig. 7. Flowchart of the drift-free modified P&O MPPT algorithm.

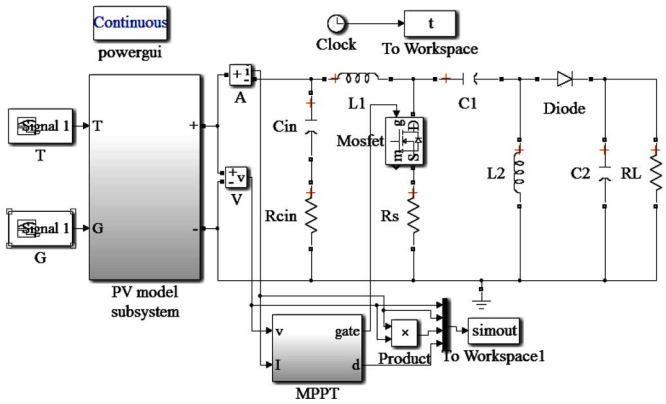

Fig. 8. MATLAB/Simulink model of simulated PV system.

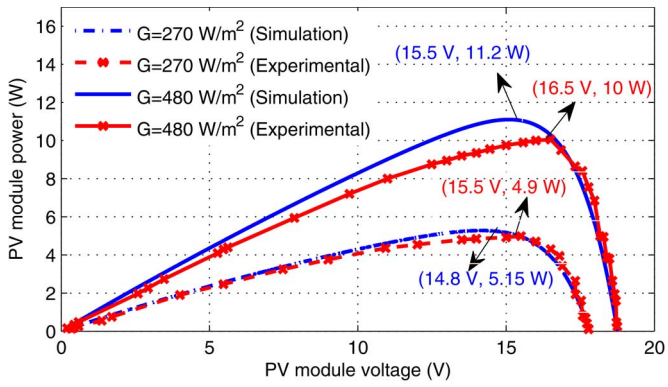

Fig. 9. Simulation and experimental P–V characteristics of the PV module for two different insolation levels.

the designed SEPIC converter used in the simulation and the experimental setup are chosen as $L_1 = 180\ \mu$H, $L_2 = 180\ \mu$H, $C_1 = 47\ \mu$F, $C_2 = 220\ \mu$F, $C_{in} = 440\ \mu$F, $f_s = 50$ kHz, and $R_L = 23\ \Omega$. The MATLAB/Simulink model of the proposed system is shown in Fig. 8. The P–V characteristics of the simulated PV module are shown in Fig. 9, and from the P–V characteristics, it can be noticed that the MPP voltages are 14.8 and 15.5 V, corresponding to the insolation level of 270 and 480 W/m^2, respectively.

A. Drift Analysis for One Step Change in Insolation

The proposed MPPT algorithm has been tested for a step change in insolation level from 270 to 480 W/m^2 at 1.01 s. The perturbation time (T_a) and the perturbation step size (ΔD) are chosen as 20 ms and 1%, respectively. The tracking waveforms with the proposed drift-free modified P&O and conventional P&O MPPT method are shown in Fig. 10, and it can be visualized that both methods are efficiently tracking

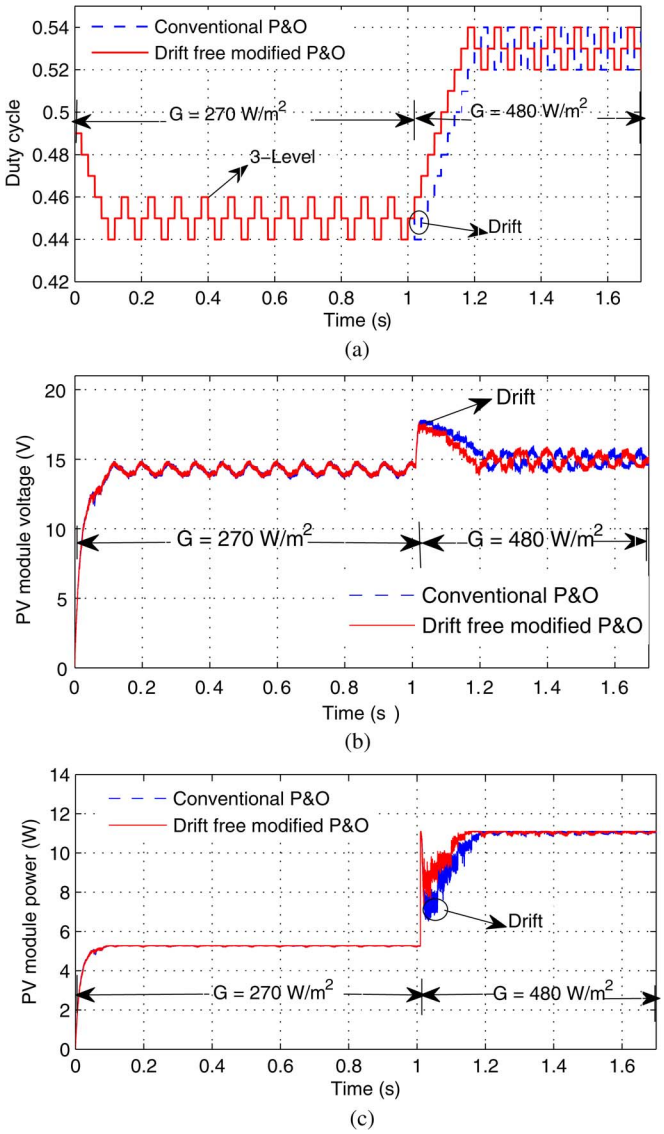

Fig. 10. With conventional and drift-free modified P&O MPPT for one time insolation change. (a) Duty cycle variation. (b) Voltage. (c) Power.

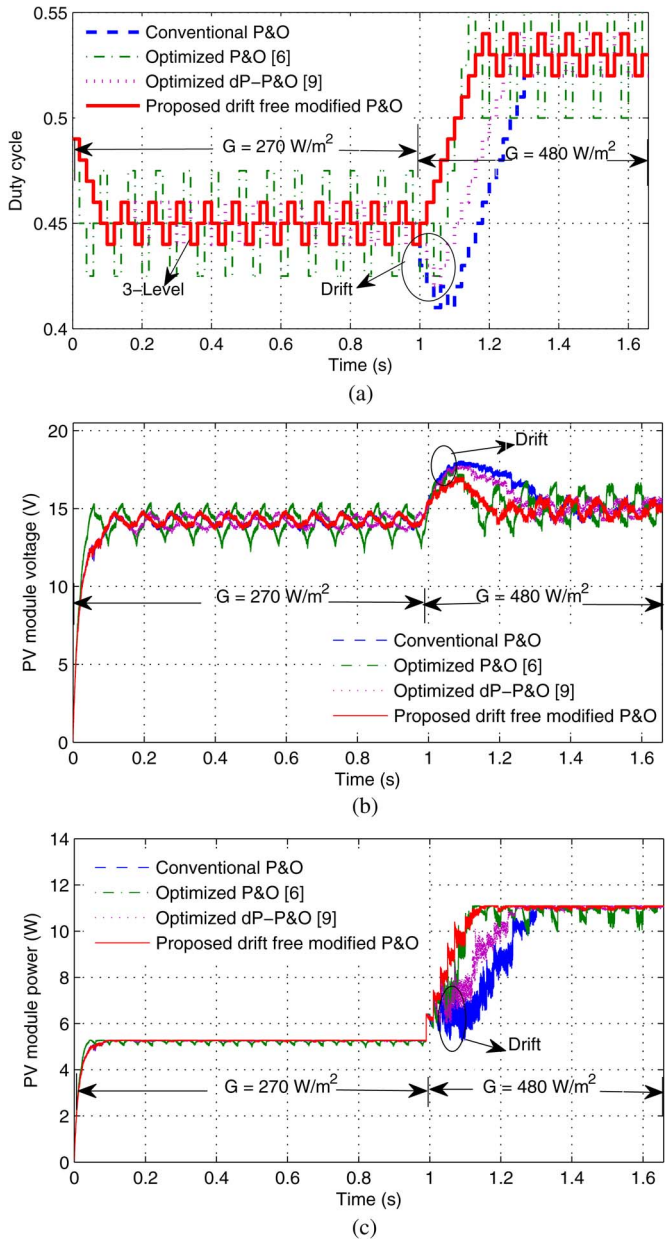

Fig. 11. With the conventional P&O, optimized P&O [6], optimized dP-P&O [9], and proposed drift-free modified P&O MPPT for rapid change in insolation. (a) Duty cycle variation. (b) Voltage. (c) Power.

the corresponding MPP, but the conventional P&O is suffering from the drift, whereas the proposed method is free from drift.

B. Drift Analysis for Rapid Increase in Insolation With Conventional P&O, Optimized P&O [6], Optimized dP-P&O [9], and Proposed Modified P&O

The drift problem is severe in case of a rapid increase in insolation. Hence, to test the performance of the proposed algorithm with respect to existing drift-free methods such as optimized P&O [6] and optimized dP-P&O [9], simulation is performed for a rapid increase in insolation of 42 W/m^2 successively five times from 270 to 480 W/m^2, and the corresponding tracking waveforms are shown in Fig. 11. To avoid the drift in case of a large change in insolation according to [6], a high value of perturbation step size (ΔD) should be chosen. The optimized P&O [6] simulation is carried out by considering $\Delta D = 2.5\%$ to avoid the drift in this case. From Fig. 11, it can be visualized that the optimized P&O [6] is able to avoid the drift provided that the value of ΔD is large, but at the same time, the power losses have been increased due to large voltage oscillations around the MPP. The other method optimized dP-P&O [9] is able to avoid the drift provided that the setting of the threshold values should meet the criteria for avoiding the drift. Moreover, the optimized dP-P&O [9] method has some disadvantages of more complexity, requirement of threshold setting, and requirement of an additional sampling at $T_a/2$ instant for every iteration. From Fig. 11, it is worth to mention that the proposed method is free from drift without any constraints on ΔD and no requirement of an additional sampling compared to the aforementioned alternative methods.

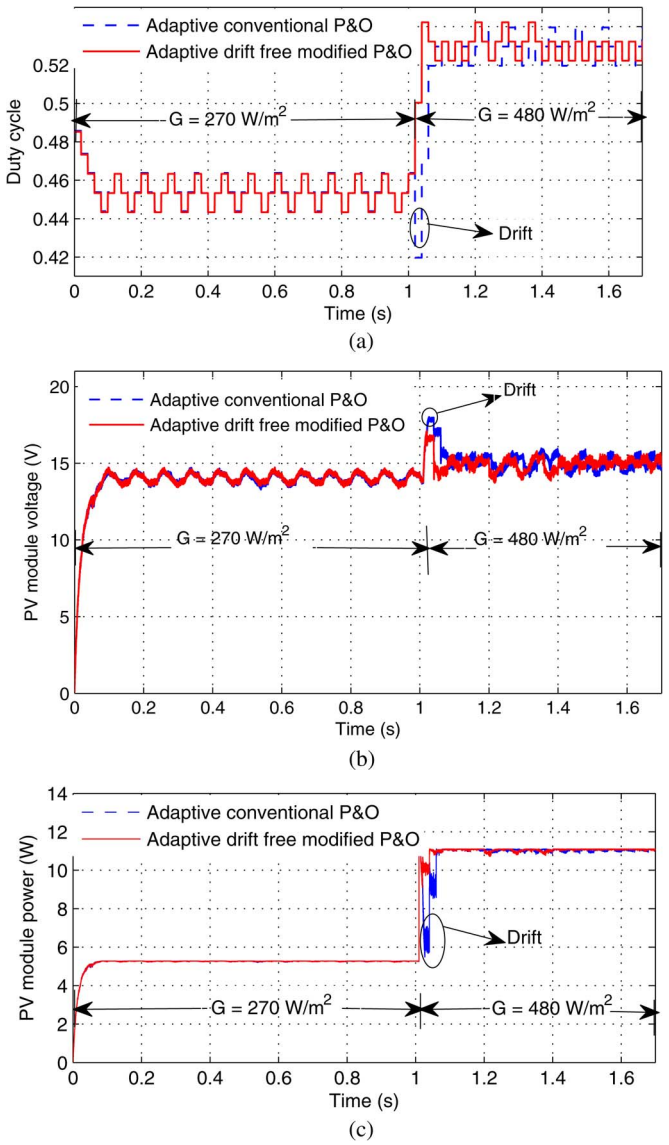

Fig. 12. Adaptive technique for conventional and drift-free modified P&O MPPT for one time insolation change. (a) Duty cycle variation. (b) Voltage. (c) Power.

C. Drift Analysis for One Step Change in Insolation With Adaptive Conventional P&O and Proposed Modified P&O

The adaptive technique with $\Delta D = M(dP/dV)$ [8], [14] has been simulated for a step change in insolation of 270–480 W/m^2 at 1.01 s with conventional P&O and drift-free modified P&O algorithm, and the corresponding tracking waveforms are shown in Fig. 12. From Fig. 12(a), it is worth to mention that the effect of drift is more with the adaptive technique applied to conventional P&O due to the large value of ΔD generated by the adaptive technique, whereas the proposed method with adaptive technique is free from drift.

The steady-state power loss calculation in case of P&O is addressed in [34] and [35]. The power loss (P_r) due to oscillations in comparison with the available maximum power $(P_{\rm mp})$ can be expressed as follows [34]:

$$\frac{P_r}{P_{\rm mp}} = \left(\frac{(\Delta V_{\rm PV})_{\rm RMS}}{V_{\rm MPP}}\right)^2 \left(1 + \frac{V_{\rm MPP}}{2av_t}\right) \qquad (12)$$

TABLE I
COMPARISON OF PROPOSED DRIFT-FREE MODIFIED P&O WITH OTHER ALTERNATIVE DRIFT-FREE METHODS

Sl.No.	Parameter	Optimized P&O [6]	Optimized dP-P&O [9]	Proposed drift free modified P&O
1	Power loss	more	less	less
2	Steady state operation	3-Level	3-Level	3-Level
3	Sampling instants per iteration	$(k-1)T_a$, kT_a	$(k-1)T_a$, $\frac{kT_a}{2}$, kT_a	$(k-1)T_a$, kT_a
4	Implementation complexity	Low	High	Low

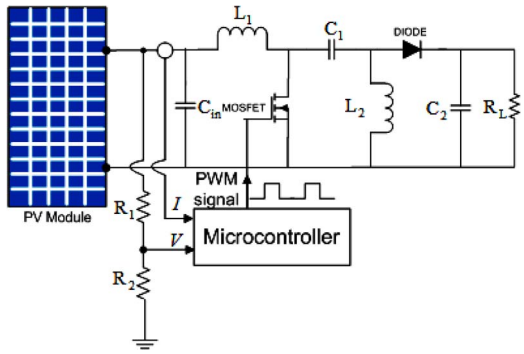

Fig. 13. Circuit model of the developed PV system.

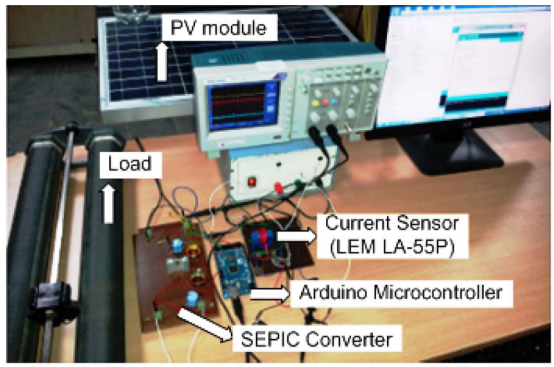

Fig. 14. Experimental setup of the developed PV system.

where $(\Delta V_{\rm PV})_{\rm RMS}$ is the rms value of steady-state voltage oscillation and $V_{\rm MPP}$ is the PV module voltage at MPP. From (12) and Fig. 11(b), it can be observed that the power loss with optimized P&O [6] is more due to large voltage oscillations compared to the optimized dP-P&O [9] and proposed drift-free modified P&O method. The comparison of the proposed drift-free modified P&O with the alternative drift-free methods such as optimized P&O [6] and optimized dP-P&O [9] is presented in Table I.

V. EXPERIMENTAL VALIDATION

To validate the functionality and performance of the proposed drift-free modified P&O MPPT technique, a prototype of the SEPIC converter and control circuit has been developed. The SEPIC converter has been constructed using the designed parameters presented in Section IV. The ARDUINO ATMEGA

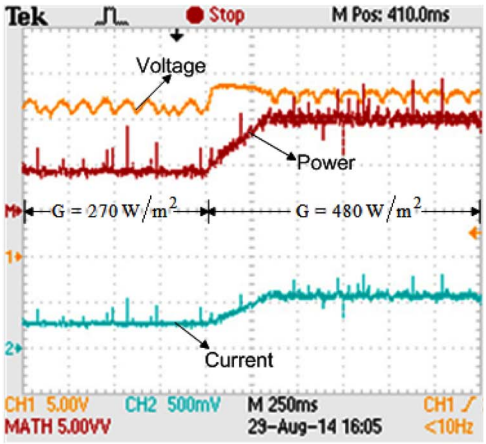

(a)

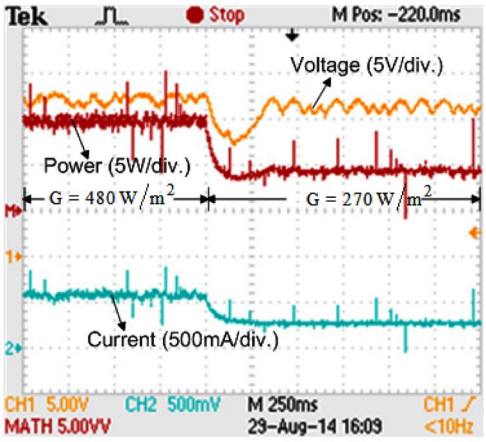

(b)

Fig. 15. Tracking waveforms with drift-free modified P&O MPPT for $\Delta D = 1\%$ and $T_a = 20$ ms. (a) For a change in solar insolation from $(G, T) = (270$ W/m^2, 43 °C) to (480 W/m^2, 48 °C). (b) For a change in solar insolation from $(G, T) = (480$ W/m^2, 48 °C) to (270 W/m^2, 43 °C).

2560 microcontroller has been used for digital implementation of the MPPT algorithm and to provide the PWM control signal to the designed SEPIC converter. The circuit model and the experimental setup of the developed system are shown in Figs. 13 and 14, respectively.

The voltage and current sensors are required to implement the P&O MPPT algorithm, and the microcontroller board cannot accept more than 5 V. Therefore, the panel voltage is sensed using the voltage divider circuit with resistances R_1 and R_2 of values 10 and 1 kΩ, respectively, and the current sensing is done using LEM LA-55P. The PV module chosen for the experimental setup having the model number ELDORA 40-P is shown in Fig. 14, and the experiment is performed using the artificial insolation with the help of halogen and incandescent lamps.

The modified P&O MPPT technique with fixed step size is tested for a step increase in insolation level of 270–480 W/m^2 and for a step decrease in insolation level of 480–to 270 W/m^2. The experimental P–V characteristics of the considered PV module at $(G, T) = (270$ W/m^2, 43 °C) and at $(G, T) = (480$ W/m^2, 48 °C) are shown in Fig. 9. From the P–V characteristics, it can be observed that the voltage and power

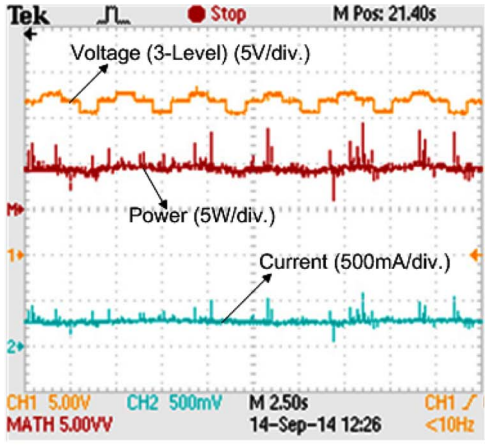

(a)

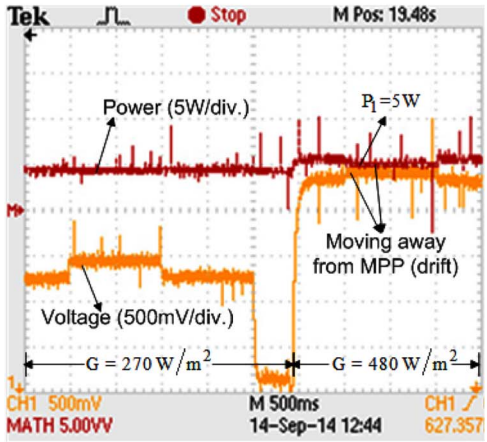

(b)

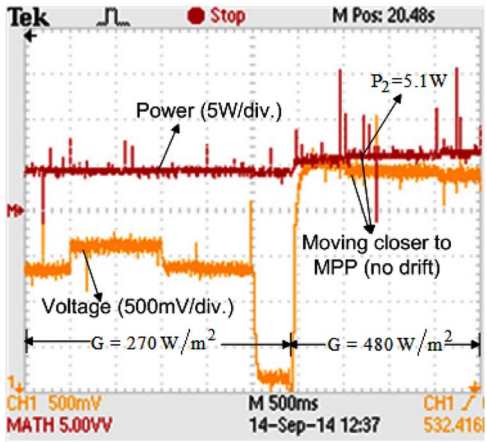

(c)

Fig. 16. Tracking waveforms with $\Delta D = 1\%$ and $T_a = 1$ s.(a) Three-level operation with drift-free modified P&O MPPT for $(G, T) = (270$ W/m^2, 43 °C). (b) Drift existence with conventional P&O for a change in solar insolation from $(G, T) = (270$ W/m^2, 43 °C) to (480 W/m^2, 48 °C). (c) Drift absence with drift-free modified P&O MPPT for a change in solar insolation from $(G, T) = (270$ W/m^2, 43 °C) to (480 W/m^2, 48 °C).

corresponding to MPP for the aforementioned insolation and temperature conditions are (15.5 V, 4.9 W) and (16.5 V, 10 W), respectively. The tracking waveforms with a fixed step size of 1% for a step increase in insolation level of 270–480 W/m^2 are shown in Fig. 15(a), and that for a step decrease in insolation

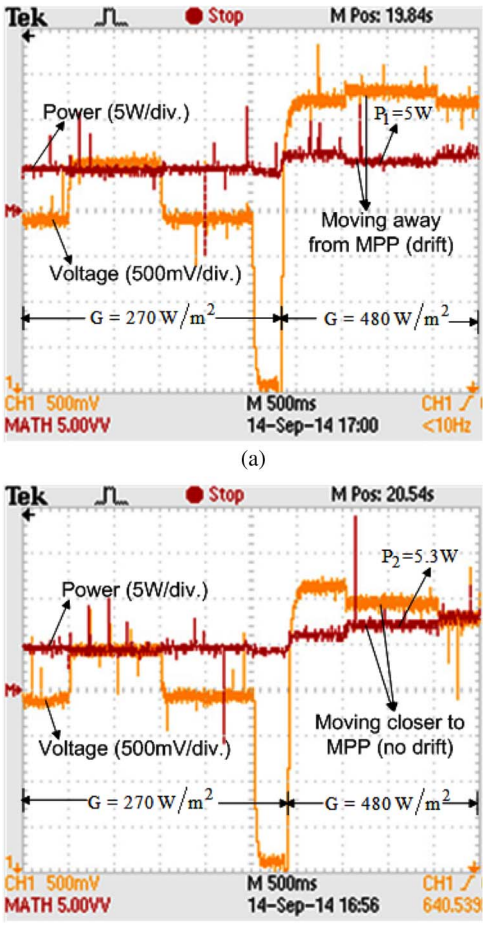

Fig. 17. Tracking waveforms with $\Delta D = 2\%$ and $T_a = 1$ s. (a) Drift existence with conventional P&O for a change in solar insolation from $(G, T) = (270$ W/m$^2, 43$ °C) to (480 W/m^2, 48 °C). (b) Drift absence with drift-free modified P&O MPPT for a change in solar insolation from $(G, T) = (270$ W/m$^2, 43$ °C) to (480 W/m^2,48 °C).

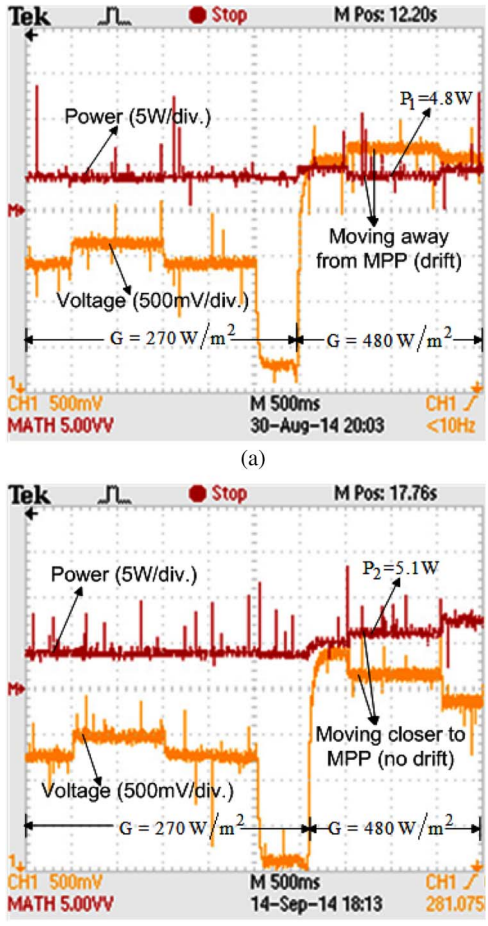

Fig. 18. Tracking waveforms with adaptive ΔD and $T_a = 1$ s. (a) Drift existence with conventional P&O for a change in solar insolation from $(G, T) = (270$ W/m$^2, 43$ °C) to (480 W/m^2, 48 °C). (b) Drift absence with drift-free modified P&O MPPT for a change in solar insolation from $(G, T) = (270$ W/m$^2, 43$ °C) to (480 W/m^2, 48 °C).

level of 480–270 W/m^2 is shown in Fig. 15(b). Fig. 15 shows that the drift-free modified P&O MPPT technique is efficiently tracking the MPP for both increase and decrease in insolation.

For clear observation of the drift problem with conventional P&O, the experiment is carried out with $T_a = 1$ s and with different $\Delta D = 1\%, 2\%$, and the corresponding results are shown in Figs. 16 and 17. The three-level steady-state operation of the P&O MPPT technique for an insolation of $(G, T) = (270$ W/m$^2, 43$ °C) is shown in Fig. 16(a). The drift analysis is carried out for a step change in insolation of $(G, T) = (270$ W/m$^2, 43$ °C) to $(G, T) = (480$ W/m$^2, 48$ °C) in between the perturbation time. From Figs. 16(b) and 17(a), it can be noticed that, for an increase in insolation, the operating voltage is increased (power is reduced) in the next perturbation and causes the conventional P&O to move away from MPP called drift, whereas with the proposed MPPT technique for the same increment in insolation, the operating voltage is decreased (power is increased) in the next perturbation as shown in Figs. 16(c) and 17(b). The drift behavior with adaptive technique has been tested with $\Delta D = M * |(V_{\rm PV} dI_{\rm PV} + I_{\rm PV} dV_{\rm PV})|$ instead of $\Delta D = M * |dP/dV|$ to avoid the possible uncertainty due to $dV \approx 0$ [17] and $T_a = 1$ s for a step change in insolation of $(G, T) = (270$ W/m$^2, 43$ °C) to $(G, T) = (480$ W/m$^2, 48$ °C) in between the perturbation time. As shown in Fig. 18(a) compared to Figs. 16(b) and 17(a), it is worth to mention that the drift effect is severe in case of the conventional adaptive P&O, whereas in case of the adaptive modified P&O, the operating point moves very closer to MPP as shown in Fig. 18(b). Thus, the proposed MPPT technique is free from drift and results in tracking time as well as power loss reduction, and it will be effective in case of a rapid increase in insolation compared to the conventional P&O MPPT technique. For evaluating the power loss with the conventional P&O, the power levels during the first T_a period after the change of insolation with the conventional P&O and proposed method are denoted as P_1 and P_2, respectively, in Figs. 16–18. As shown in Fig. 16(b), the conventional P&O is able to operate at a power level of $P_1 = 5$ W during the first perturbation period immediate to the change of insolation, whereas the proposed method is able to operate at the power level of $P_2 = 5.1$ W as shown in Fig. 16(c) because the proposed method is free from drift. The difference in power levels is more for a high value of ΔD and also for the adaptive

TABLE II
OBSERVATION OF POWER AND ENERGY LOSS WITH CONVENTIONAL P&O COMPARED TO PROPOSED METHOD DUE TO DRIFT PHENOMENA FROM EXPERIMENTAL FIGS. 16–18

Sl.No.	perturbation step size (ΔD)	Power loss (W)	Energy loss (J)
1	1%	$P_2 - P_1 \approx 0.1$	$\approx 0.1T_a$
2	2%	$P_2 - P_1 \approx 0.3$	$\approx 0.3T_a$
3	Adaptive ($M\frac{dP}{dV}$)	$P_2 - P_1 \approx 0.3$	$\approx 0.3T_a$

case as shown in Figs. 17 and 18. The power loss $(P_2 - P_1)$ and energy loss $((P_2 - P_1)T_a)$ with the conventional P&O compared to the proposed method due to the drift phenomena observed from the experimental results shown in Figs. 16–18 are presented in Table II. From Table II, it is worth to mention that, over a 25-year life cycle of a PV system, a considerable amount of energy gain can be achieved with the proposed drift-free modified P&O MPPT method for a large-scale PV system.

VI. CONCLUSION

In this paper, the drift phenomena for the widely used P&O MPPT algorithm have been thoroughly discussed, and then, a modification to the existing algorithm has been proposed to avoid the drift. The basic principle of the algorithm is to use an extra checking condition (ΔI) in the traditional P&O algorithm to avoid the drift, and the mathematical justification of checking this extra condition is also proved. The simulation and experimental validations of the proposed method are done by considering the SEPIC converter topology with direct duty ratio control. The algorithm has been validated by means of numerical simulations, considering the PV panel that has been experimentally identified and characterized. Moreover, laboratory tests have been performed on a low-power solar panel to validate the effectiveness of the proposed algorithm. The simulation and experimental results prove that the proposed modified P&O MPPT technique is free from drift and is accurately tracking the maximum power from the PV panel. The proposed algorithm improves the efficiency of the PV system by gaining the extra power during drift compared to the conventional P&O algorithm. A considerable amount of energy gain can be achieved over the life cycle of the PV panel by using the proposed method.

REFERENCES

[1] Y. T. Tan, D. S. Kirschen, and N. Jenkins, "A model of PV generation suitable for stability analysis," *IEEE Trans. Energy Convers.*, vol. 19, no. 4, pp. 748–755, Dec. 2004.

[2] W. D. Soto, S. A. Klein, and W. A. Beckman, "Improvement and validation of a model for photovoltaic array performance," *Solar Energy*, vol. 80, no. 1, pp. 78–88, Jan. 2006.

[3] M. G. Villalva, J. R. Gazoli, and E. R. Filho, "Comprehensive approach to modeling and simulation of photovoltaic arrays," *IEEE Trans. Power Electron.*, vol. 24, no. 5, pp. 1198–1208, May 2009.

[4] M. A. S. Masoum, H. Dehbonei, and E. F. Fuchs, "Theoretical and experimental analyses of photovoltaic systems with voltage and current-based maximum power-point tracking," *IEEE Trans. Energy Convers.*, vol. 17, no. 4, pp. 514–522, Dec. 2002.

[5] W. Xiao and W. G. Dunford, "A modified adaptive hill climbing MPPT method for photovoltaic power systems," in *Proc. IEEE PESC*, 2004, pp. 1957–1963.

[6] N. Femia, G. Petrone, G. Spagnuolo, and M. Vitelli, "Optimization of perturb and observe maximum power point tracking method," *IEEE Trans. Power Electron.*, vol. 20, no. 4, pp. 963–973, Jul. 2005.

[7] N. Femia, D. Granozio, G. Petrone, G. Spagnuolo, and M. Vitelli, "Predictive and adaptive MPPT perturb and observe method," *IEEE Trans. Aerosp. Electron. Syst.*, vol. 43, no. 3, pp. 934–950, Jul. 2007.

[8] A. Pandey, N. Dasgupta, and A. K. Mukerjee, "High-performance algorithms for drift avoidance and fast tracking in solar MPPT system," *IEEE Trans. Energy Convers.*, vol. 23, no. 2, pp. 681–689, Jun. 2008.

[9] D. Sera, R. Teodorescu, J. Hantschel, and M. Knoll, "Optimized maximum power point tracker for fast-changing environmental conditions," *IEEE Trans. Ind. Electron.*, vol. 55, no. 7, pp. 2629–2637, Jul. 2008.

[10] L. Piegari and R. Rizzo, "Adaptive perturb and observe algorithm for photovoltaic maximum power point tracking," *IET Renew. Power Gener.*, vol. 4, no. 4, pp. 317–328, Jul. 2010.

[11] M. A. Algendy, B. Zahawi, and D. J. Atkinson, "Assessment of perturb and observe MPPT algorithm implementation techniques for PV pumping applications," *IEEE Trans. Sustain. Energy*, vol. 3, no. 1, pp. 21–33, Jan. 2012.

[12] Y. Jiang, J. A. A. Qahouq, and T. A. Haskew, "Adaptive step size with adaptive-perturbation-frequency digital MPPT controller for a single-sensor photovoltaic solar system," *IEEE Trans. Power Electron.*, vol. 28, no. 7, pp. 3195–3205, Jul. 2013.

[13] K. L. Lian, J. H. Jhang, and I. S. Tian, "A maximum power point tracking method based on perturb-and-observe combined with particle swarm optimization," *IEEE J. Photovoltaics*, vol. 4, no. 2, pp. 626–633, Mar. 2014.

[14] F. Liu, S. Duan, B. Liu, and Y. Kang, "A variable step size INC MPPT method for PV systems," *IEEE Trans. Ind. Electron.*, vol. 55, no. 7, pp. 2622–2628, Jul. 2008.

[15] S. B. Kjaer, "Evaluation of the hill climbing and the incremental conductance maximum power point trackers for photovoltaic power systems," *IEEE Trans. Energy Convers.*, vol. 27, no. 4, pp. 922–929, Dec. 2012.

[16] M. A. Algendy, B. Zahawi, and D. J. Atkinson, "Assessment of the incremental conductance maximum power point tracking algorithm," *IEEE Trans. Sustain. Energy*, vol. 4, no. 1, pp. 108–117, Jan. 2013.

[17] G. C. Hsieh, H. I. Hsieh, C. Y. Tsai, and C. H. Wang, "Photovoltaic power-increment-aided incremental-conductance MPPT with two-phased tracking," *IEEE Trans. Power Electron.*, vol. 28, no. 6, pp. 2895–2911, Jun. 2013.

[18] K. S. Tey and S. Mekhilef, "Modified incremental conductance algorithm for photovoltaic system under partial shading conditions and load variation," *IEEE Trans. Ind. Electron.*, vol. 61, no. 10, pp. 5384–5392, Oct. 2014.

[19] Q. Mei, M. Shan, L. Liu, and J. M. Guerrero, "A novel improved variable step-size incremental-resistance MPPT method for PV systems," *IEEE Trans. Ind. Electron.*, vol. 58, no. 6, pp. 2427–2434, Jun. 2011.

[20] T. Esram, J. W. Kimball, P. T. Krein, P. L. Chapman, and P. Midya, "Dynamic maximum power point tracking of photovoltaic arrays using ripple correlation control," *IEEE Trans. Power Electron.*, vol. 21, no. 5, pp. 1282–1291, Sep. 2006.

[21] A. A. Nabulsi and R. Dhaouadi, "Efficiency optimization of a DSP-based standalone PV system using fuzzy logic and dual-MPPT control," *IEEE Trans. Ind. Informat.*, vol. 8, no. 3, pp. 573–584, Aug. 2012.

[22] Syafaruddin, E. Karatepe, and T. Hiyama, "Artificial neural network polar coordinated fuzzy controller based maximum power point tracking control under partially shaded conditions," *IET Renew. Power Gener.*, vol. 3, no. 2, pp. 239–253, Jun. 2009.

[23] K. Ishaque and Z. Salam, "A deterministic particle swarm optimization maximum power point tracker for photovoltaic system under partial shading condition," *IEEE Trans. Ind. Electron.*, vol. 60, no. 8, pp. 3195–3206, Aug. 2013.

[24] H. Renaudineau *et al.*, "A PSO-based global MPPT technique for distributed PV power generation," *IEEE Trans. Ind. Electron.*, vol. 62, no. 2, pp. 1047–1058, Feb. 2015.

[25] E. Bianconi *et al.*, "A fast current-based MPPT technique employing sliding mode control," *IEEE Trans. Ind. Electron.*, vol. 60, no. 3, pp. 1168–1178, Mar. 2013.

[26] E. Mamarelis, G. Petrone, and G. Spagnuolo, "Design of a sliding mode controlled SEPIC for PV MPPT applications," *IEEE Trans. Ind. Electron.*, vol. 61, no. 7, pp. 3387–3398, Jul. 2014.

[27] D. P. Hohm and M. E. Ropp, "Comparative study of maximum power point tracking algorithms," *Progress Photovolt: Res. Appl.*, vol. 11, no. 1, pp. 47–62, Jan. 2003.

[28] V. Salas, E. Olias, A. Barrado, and A. Lazaro, "Review of the maximum power point tracking algorithms for stand-alone photovoltaic systems,"

Solar Energy Mater. Solar Cells, vol. 90, no. 11, pp. 1555–1578, Jul. 2006.
[29] T. Esram and P. L. Chapman, "Comparison of photovoltaic array maximum power point tracking techniques," *IEEE Trans. Energy Convers.*, vol. 22, no. 2, pp. 439–449, Jun. 2007.
[30] M. A. G. de Brito, L. Galotto, L. P. Sampaio, G. A. e Melo, and C. A. Canesin, "Evaluation of the main MPPT techniques for photovoltaic applications," *IEEE Trans. Ind. Electron.*, vol. 60, no. 3, pp. 1156–1167, Mar. 2013.
[31] D. Sera, L. Mathe, T. Kerekes, S. V. Spataru, and R. Teodorescu, "On the perturb-and-observe and incremental conductance MPPT methods for PV systems," *IEEE J. Photovoltaics*, vol. 3, no. 3, pp. 1070–1078, Jul. 2013.
[32] H. S.-H. Chung, K. K. Tse, S. Y. R. Hui, C. M. Mok, and M. Ho, "A novel maximum power point tracking technique for panels using a SEPIC or Cuk converter," *IEEE Trans. Power Electron.*, vol. 18, no. 3, pp. 717–724, May 2003.
[33] A. K. Abdelsalam, A. M. Massoud, S. Ahmed, and P. N. Enjeti, "High-performance adaptive perturb and observe MPPT technique for photovoltaic based microgrids," *IEEE Trans. Power Electron.*, vol. 26, no. 4, pp. 1010–1021, Apr. 2011.
[34] C. R. Sullivan, J. J. Awerbuch, and A. M. Latham, "Decrease in photovoltaic power output from ripple: Simple general calculation and the effect of partial shading," *IEEE Trans. Power Electron.*, vol. 28, no. 2, pp. 740–747, Feb. 2013.
[35] F. Paz and M. Ordonez, "Zero oscillation and irradiance slope tracking for photovoltaic MPPT," *IEEE Trans. Ind. Electron.*, vol. 61, no. 11, pp. 6138–6147, Nov. 2014.

Muralidhar Killi received the B.Tech. degree in electronics and communication engineering from V. R. Siddhartha Engineering College, Vijayawada, India, in 2008 and the M.Tech. degree in electrical engineering from the National Institute of Technology, Rourkela, India, in 2012, where he is currently working toward the Ph.D. degree in electrical engineering.

His areas of research interest include modeling, analysis, and control of photovoltaic systems and power electronic converter circuits.

Susovon Samanta (M'11) received the B.E. degree in electrical engineering from the Regional Engineering College, Durgapur, India, in 1998, the M.E. degree in electrical engineering from Jadavpur University, Jadavpur, India, in 2003, and the Ph.D. degree in electrical engineering from the Indian Institute of Technology, Kharagpur, India, in 2012.

From 2003 to 2004, he was a Lecturer with Birla Institute of Technology, Mesra, India. In 2009, he joined the National Institute of Technology, Rourkela, India, where he is currently an Assistant Professor. His research interests are in the analysis, modeling, and control of power converters used in various areas such as PV, EV, and space applications.